Nanoscale Advances

ROYAL SOCIETY OF CHEMISTRY

PAPER

View Article Online
View Journal | View Issue

Cite this: *Nanoscale Adv.*, 2020, **2**, 3494

A biomimetic yeast shell vaccine coated with layered double hydroxides induces a robust humoral and cellular immune response against tumors†

Dong-qun Liu,‡[ab] Shuai Lu,‡[a] Lun Zhang,[ab] Ling-xiao Zhang,[ab] Mei Ji,[ab] Xiao-Ge Liu,[ab] Zhuo Yu*[c] and Rui-tian Liu*[a]

Enhancing both the humoral and cellular immune response for tumor vaccination remains a challenge. Inspired by natural pathogen structures, we took β-glucan particles derived from a baker's yeast cell shell (YS) as a vaccine carrier and danger signal for dendritic cells (DCs), and coated the YS with catanionic layered double hydroxides (LDH) by electrostatic adsorption to form a biomimetic yeast cell particle (YSL). Our experimental results showed that the YSL vaccine efficiently targeted antigen-presenting cells (APCs) and remarkably enhanced antigen cross-presentation, and strongly improved the activation and maturation of DCs. Moreover, the YSL vaccine elicited an extremely high antibody titer and strong antigen-specific cytotoxic T lymphocyte together with mixed Th1/Th17 cellular immune responses and induced marked prophylactic and therapeutic effects against E.G7-OVA tumors in mouse models. These results suggest that YSL, integrating a yeast shell to mimic natural pathogens and LDH with high antigen-loading capacity and lysosome escape, is a promising tumor vaccine platform for rapid, effective and strong induction of both humoral and cellular immune responses.

Received 30th March 2020
Accepted 25th June 2020

DOI: 10.1039/d0na00249f

rsc.li/nanoscale-advances

Introduction

Vaccination is one of the most useful and cost-effective methods to prevent or fight against tumors as well as other diseases.[1,2] An efficient tumor vaccine should induce an extensive humoral response and cellular immune response, including $CD8^+$ cytotoxic T cell (CTL), $CD4^+$ Th1 or Th17 cell responses, with the aid of an adjuvant.[3–5] However, the most commonly used adjuvant, aluminum salt (alum), can only generally elicit a strong antibody response with a Th2 bias,[6] and few adjuvants licensed for human administration have been able to generate enough cellular immune response.[7] New strategies with the ability to enhance both humoral and cellular immune responses remain a priority for the development of therapeutic tumor vaccines.

As a generally recognized as safe (GRAS) particulate system approved by the FDA, yeast shell walls (β-glucan particles) are particularly attractive as vaccine adjuvants and antigen carriers.[6,8] The yeast shell has a perfect natural size of 2–4 μm, inducing specific uptake by phagocytes such as DCs and macrophages rather than most non-phagocytic cells, and avoiding the risk of antigen uptake and presentation by non-APCs.[9] Moreover, DCs and macrophages recognize the β-1,3-D-glucan backbone structure through dectin1 and toll-like receptors (TLRs), such as TLR-2 and TLR-6,[10,11] inducing maturation of APCs and activation of the mixed Th1 and Th17 adaptive immune responses.[12,13] However, the antigen loading capacity of yeast shells is low and the loaded antigen can easily be released before reaching the APCs.

As antigen protectors and carriers, layered double hydroxide (LDH) nanomaterials have attracted increasing attention and have been investigated as adjuvants to enhance the immune responses to antigens.[14–16] The most studied MgAl-LDH NPs, with the general formula of $[M1-x^{2+}Mx^{3+}(OH)_2]^{x+}(An-)_{x/n}\cdot mH_2O$, carry positive charges, which can be used to electrostatically load negatively-charged biological molecules (such as oligonucleotides, DNA, RNA, and proteins) for delivery to mammalian cells to enhance cellular uptake due to its good biocompatibility, high payload loading capacity, easy and low-cost preparation.[17,18] Moreover, these particles not only facilitate the access of antigens to APCs but also alter intercellular trafficking.[19,20] Elaborately designed LDH carriers have been demonstrated to evade lysosome degradation and stimulate

[a]National Key Laboratory of Biochemical Engineering, Institute of Process Engineering, Chinese Academy of Sciences, Haidian District, Beijing 100190, China. E-mail: rtliu@ipe.ac.cn; Fax: +86 10 82545025; Tel: +86 10 82545017

[b]School of Chemical Engineering, University of Chinese Academy of Science, Beijing 100049, China

[c]Beijing Tsinghua Changgung Hospital, Changping District, Beijing. 102218, China. E-mail: yza02214@btch.edu.cn; Fax: +86 10 56118500; Tel: +86 10 56119544

† Electronic supplementary information (ESI) available. See DOI: 10.1039/d0na00249f

‡ These authors equally contributed to this work.

cross-presentation of internalized antigen.[21,22] The alkalinity of MgAl–LDH material maintains the endosomal pH at around 6 through a minor dissolution of LDH, which increases osmotic pressure within the endosome and ultimately leads to endosome rupture, providing access to subsequent antigen cross-presentation.[23] Thus, LDH has been investigated as a carrier to enhance immune responses to antigens.[24–26] Nevertheless, LDH mainly induces a humoral response with a low Th1 cellular immune response, limiting its clinical use as a tumor vaccine adjuvant.[14]

Inspired by natural pathogen structures with repetitive epitope arrangements on the microorganism surface,[15] we have developed a novel composite immunotherapeutic agent, YSL, using yeast shell derived β-glucan particles as a carrier which were coated with positively charged LDH through electrostatic interactions to load antigen on the surface (Fig. 1) and then assessed its prophylactic and therapeutic effects on tumors after a tumor antigen was absorbed on YSL particles.

Experimental section

Materials

Ovalbumin was obtained from Sigma-Aldrich (St. Louis, MO, USA). Brefeldin A solution and the following fluorescence-labeled antibodies, mouse PE/Cy7-anti-CD3 antibody, FITC-anti-CD4 antibody, FITC-anti-CD8a antibody, Percp-anti-CD8a antibody, PE-anti-IL4 antibody and APC-anti-IFN-γ antibody, were purchased from BioLegend (San Diego, CA). LysoTracker Red DND-99, RPMI medium 1640 basic, fetal bovine serum and penicillin streptomycin were purchased from Thermo Fisher Scientific (MA, USA). Mouse cytokine ELISA kits were obtained from BioLegend (San Diego, CA, USA). Recombinant mouse granulocyte-macrophage colony-stimulating factor (GM-CSF) and interleukin (IL)-4 were purchased from PeproTech (Rocky Hill, USA).

Cell culture and animals

All animal procedures were performed in accordance with the China Public Health Service Guide for the Care and Use of Laboratory Animals and approved by the Animal Care and Use Committee of the Institute of Process Engineering, Chinese Academy of Sciences.

6–8 week-old C57BL/6 female mice were obtained from Beijing HFK Bioscience (Beijing, China) and maintained with access to food and water ad libitum in a colony room kept at 22 ± 2 °C and 50 ± 5% humidity under a 12 : 12 light/dark cycle.

Mouse E.G7-OVA cells were gifted by Prof. Guanghui Ma from the State Key Laboratory of Biochemical Engineering, Institute of Process Engineering, Chinese Academy of Sciences. Cells were maintained in 1640 medium supplemented with 10% fetal bovine serum, 0.4 mg mL^{-1} G418, 100 U mL^{-1} penicillin and 100 μg mL^{-1} streptomycin (Invitrogen, Carlsbad, CA) at 37 °C and 5% CO_2. Mouse RF33.70 T hybridoma cells were kindly provided by Prof. Yuhong Xu from School of Life Sciences and Biotechnology, Shanghai Jiao Tong University, Shanghai,

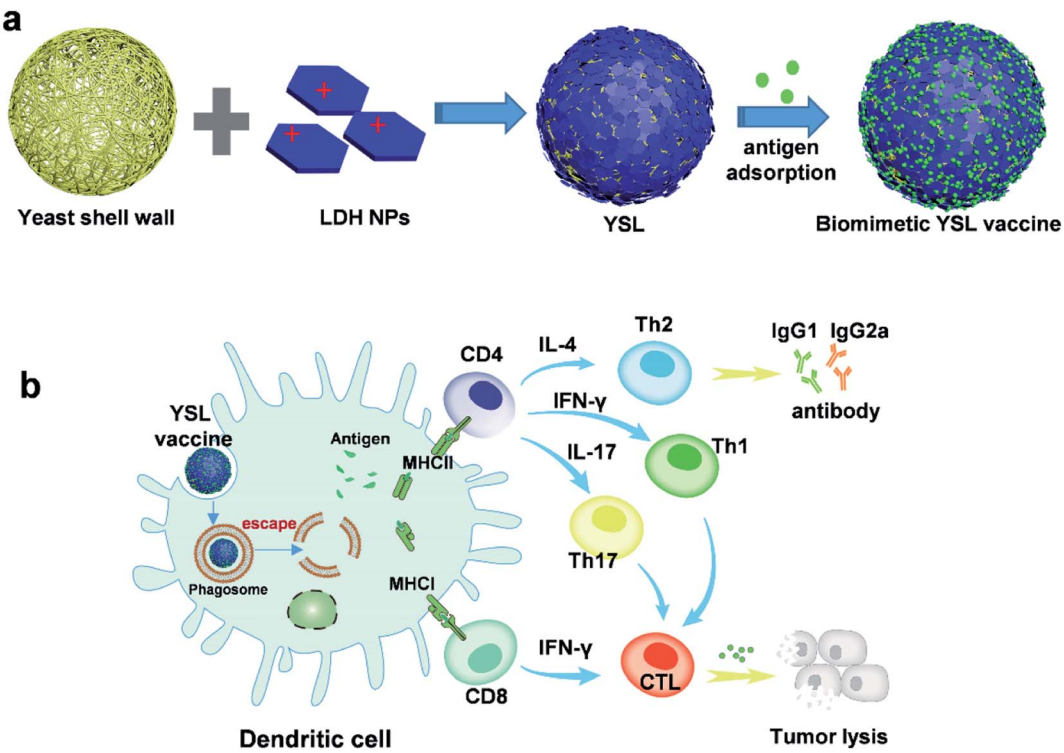

Fig. 1 Schematic illustration of the LDH nanoparticle-coated yeast shell vaccine and immune activation. (a) Schematic illustration of the construction of biomimetic YSL vaccine. (b) Schematic illustration of intracellular tracking of YSL vaccine and antigen-specific humoral and cellular immune response induced by YSL vaccine.

China. These cells were maintained in RPMI-1640 culture medium with 10% fetal bovine serum and antibiotics.

Mouse bone marrow-derived dendritic cells (BMDCs) were prepared as described previously.[16] Briefly, bone marrow cells were isolated from 6 week-old C57BL/6 mice, residual tissue was removed using a 70 μm nylon cell strainer (BD Bioscience, Franklin Lakes, NJ, USA), and the red blood cells were lysed using RBC Lysing Buffer (BioLegend). Bone marrow cells were plated in 6-well culture plates (10^6 cells per mL, 5 mL per well) in RPMI-1640 complete medium supplemented with 20 ng mL^{-1} GM-CSF and 20 ng mL^{-1} IL-4. The medium was replaced every 2 days with fresh cytokine-supplemented medium. On day 6 after plating, aggregates of immature DCs were collected and used for subsequent experiments. The content of $CD11c^+$ cells in these preparations was detected with an Accuri C6 flow cytometer (BD Biosciences, USA).

Preparation of yeast shell particles

Yeast shell particles (YS) were prepared from Baker's yeast by a slight modification of the alkaline and acidic extraction method described previously,[9] followed by either lyophilization or spray-drying. Briefly, the yeast cells were suspended in 200 mL of 1 M NaOH solution and stirred for 30 min at 60 °C. The resulting material was heated to 80 °C for 60 min and then centrifuged at 2000*g* for 10 min. The sediment was washed with water with the pH adjusted to 4–5 by HCl and incubated at 55 °C for 60 min. The alkali insoluble solids were then collected by centrifugation, washed with water, and subsequently 4 times with isopropanol and then twice with 40 mL of acetone. To overcome particle aggregation, the semisolid YS (after acetone washing) was sonicated (Sonics, UK) for 5 min in water using an ultrasonic output frequency of 20 kilohertz per second at 192 watts and then homogenized (IKATM) at 10 000 rpm for 10 min. The suspension was finally freeze-dried using a lyophilizer (CHRIST, Germany).

Preparation and characterization of LDH

MgAl–Cl–LDH nanoparticles were synthesized under sterile conditions, as previously described with slight modifications.[24] All operations in this study were undertaken under N_2 atmosphere protection and ddH_2O was boiled three times to remove atmospheric CO_2. To prepare the LDH, 10 mL of salt solution (700 mM $MgCl_2$ and 300 mM $AlCl_3$) was rapidly added to a 40 mL solution containing 450 mM NaOH under vigorous stirring. After 10 min, the LDH slurry was separated by centrifugation at 4500*g* and washed twice with deionized water. The slurry was manually dispersed in deionized water (40 mL) and subsequently transferred to a stainless steel autoclave with a Teflon lining (Parr Acid Digestion Vessels) for hydrothermal treatment at 100 °C for 16 h.

Direct assembly of LDH on the surface of yeast shell

For the preparation of YS-LDH particles, 5 mg of YS particles were resuspended in water (1.0 mL). This suspension was mixed with 10 mg of LDH in 1 mL of water. The resultant mixture was ultrasonicated at room temperature for 30 min. Then the LDH/YS composite particles were centrifuged at 3000 rpm for 5 min, and the supernatant was removed.

For antigen loading, 1 mg of YS-LDH microspheres in 0.1 mL of water was mixed with protein OVA (10 mg mL^{-1}, 10 μL) for 30 min at room temperature with shaking. The supernatant was removed by centrifugation, and the particles were washed with water three times. The loading capacity was calculated by measuring unbound OVA in the supernatant.

Intracellular trafficking of YSL particles

To monitor the DC uptake of the YSL-OVA particles, the BMDCs were placed in a 24-well plate and incubated with FAM-OVA alone and YSL-OVA at a ratio of 1 : 10 (cell : YS) at 37 °C in 5% CO_2 for 0.5–24 h. The BMDCs were washed twice with PBS, and the fluorescence in BMDCs was analyzed with a flow cytometer and measured on a confocal scanning laser microscope (LSM780, Zeiss, Germany). To detect the ability of the YSLs to escape from phagosomes in BMDCs, the FAM-labeled OVA was used in YSL-OVA preparation. The BMDCs were incubated with YSL-OVA particles for 4, 8 and 12 h, respectively. 50 nM Lyso-Track Red was then added and co-incubated for 30 min. The cells were rinsed twice, fixed with fresh 4% paraformaldehyde, treated with 10 μg mL^{-1} DAPI in PBS for 15 min, and then observed on a confocal scanning laser microscope (LSM780, Zeiss, Germany).

The cytotoxicity of YSL particles was analyzed with an MTT assay. BMDCs were seeded in 96-well plates at a concentration of 2×10^4 cells per well, and then the cells were incubated with various ratios of YSL-OVA to cell for 24 h. Then, MTT (0.5 mg mL^{-1}) was added to each well for another 4 h at 37 °C, and 100 μL of solution containing 10% SDS, 5% isobutanol, and 0.012 mol L^{-1} HCl was added to dissolve the crystals. The absorbance at 570 nm was measured on a microplate reader (EXL-800; Bio-Tek, Winooski, VT, USA).

Ability of YSL particles to induce BMDC maturation and cytokine secretion

Immature BMDC cells were incubated with PBS, OVA (2 μg mL^{-1}), LDH-OVA (LDH : OVA = 16 : 1, containing 2 μg OVA per mL), YSL (YSL : cell = 10 : 1), YSL-OVA (YSL : cell = 10 : 1 containing 2 μg OVA per mL) at 37 °C for 48 h. Cells were then harvested and stained with PE-Cy7-labeled CD11c, PE-labeled anti-mouse CD40, FITC-labeled anti-mouse CD80, FITC-labeled anti-mouse MHCII or APC-labeled anti-mouse CD86 monoclonal antibodies (BioLegend, San Diego, CA), respectively. Expression levels of co-stimulators on the surface of BMDCs, such as CD40, CD80, MHCII and CD86, were assayed using an Accuri C6 flow cytometer. The levels of inflammatory cytokines in the culture medium, including IFN-γ, IL-6, TNF-α and IL-12, were assayed using an enzyme-linked immunosorbent assay (ELISA) kits (BioLegend, San Diego, CA).

In vitro antigen processing and RF33.70 cell activation by YSL-OVA stimulation

Immature BMDCs were incubated at 37 °C for 24 h with free OVA, LDH-OVA (ratio = 16 : 1) or YSL-OVA (containing 10^6 YS)

over the indicated OVA concentration range, and then RF33.70 cells were co-incubated for 24 hours with dendritic cells at a ratio of 5 : 1. The expression of SIINFEKL-MHCI$^+$ of DCs was detected by flow cytometry. The amount of IL-2 from activated RF33.70 T hybridoma cells was determined by ELISA (Neobioscience Technology Co, Ltd).

Biodistribution of YSLs in mice and recruitment of monocytes

C57BL/6 mice received subcutaneous injections of YSL-OVA and LDH-OVA particles containing Cy5-OVA (20 μg OVA) in the inguinal region. The control group mice were injected with the same amount of Cy5-OVA alone. The fluorescence in the mice was detected at 0 h to 48 h to determine the distribution of YSL particles using the *In vivo* Imaging System FX Pro (KODAK, USA). To detect the trail of DCs and inflammation stimulated by YSLs, mice were sacrificed 4 days post-yeast administration. Draining lymph nodes were extracted and digested into a single cell suspension to detect the expression SIINFEKL-MHCI$^+$ of recruited DCs. The antigen depots were homogenized to detect inflammation cytokines. Meanwhile, some were histologically evaluated with hematoxylin and eosin (H&E) staining to detect APC recruitment.

Animal immunization and *in vivo* assay of humoral immune responses

C57BL/6 mice were immunized subcutaneously in the inguinal region with YSL-OVA particles (1.0 mg particles per mouse, containing 50 μg OVA per mouse) twice at two-week intervals, with soluble OVA (50 μg OVA per mouse), YSL (1.0 mg per mouse), and LDH-OVA (50 μg OVA per mouse) used as controls. Seven days after the last immunization, blood was collected for antibody titer determination with the ELISA kit.

For the antibody titer determination with ELISA, OVA was diluted with 20 mM PBS (10 μg mL^{-1}) and coated onto 96-well plates at 4 °C overnight. The plates were washed three times in PBS containing 0.1% Tween 20 (PBST) and blocked with 3% BSA solution at 37 °C for 2 h. After washing three times with PBST, serial two-fold dilutions of sera were performed, and the plates were incubated at room temperature for 2 h. The plates were washed 6 times and reacted with a 5000-fold dilution of horseradish peroxidase (HRP)-labeled goat anti-mouse IgG, IgG1 and IgG2a antibodies (Thermo Fisher Scientific MA, USA) at room temperature for 1 h. Finally, the plates were washed 8 times and developed with TMB substrate (100 μL per well) for 15 min, the chromogenic reaction of which was stopped by adding H_2SO_4. The absorbance was measured on a SpectraMax M5 microplate reader at 450 nm.

Tumor challenge and evaluation of anti-tumor activity

For prophylactic vaccination against E.G7-OVA tumor challenge, mice were primed with OVA proteins, LDH-OVA particles or YSL-OVA particles and boosted again 14 days later. Mice immunized with PBS and YSL were used as the negative controls. At day 28, the vaccinated mice were subcutaneously challenged with 1×10^6 E.G7-OVA tumor cells in the right flank. Tumor sizes were measured with a caliper every other day for 24 days. Tumor volume was calculated using the formula $1/2\times$ length $\times$ width^2. The tumor volumes of deceased mice were not included after the day of death. The survival times were recorded throughout the tumor challenge.

To test the therapeutic effects of these vaccines against E.G7-OVA tumors, mice were subcutaneously challenged with 1×10^6 E.G7-OVA cells in the right flank. Mice were vaccinated with YSL-OVA particles (1.0 mg/mouse, containing 50 μg OVA per mouse) on days 4 and 11 (booster injection) after E.G7-OVA cell transplantation. Tumor sizes were measured and calculated as previously mentioned.

In vivo CTL assay

The *in vivo* assay was performed on C57BL/6 mice seven days after the vaccination according to the previous protocol with slight modification.[27] Splenocytes from naive C56BL/6 mice were collected and pulsed with either 10 μM $OVA_{257-264}$ peptide or 1640 complete media at 37 °C for 2 h. The $OVA_{257-264}$ peptide-pulsed cells or 1640 complete media treated cells were labeled with 4 and 0.4 μM CFSE, respectively. Equal amounts of CFSE^{high} (peptide-pulsed cells) and CFSE^{low} (media-treated cells) were mixed and injected intravenously into the control or immunized mice. After 18 h, splenocytes from these treated mice were collected and subjected to flow cytometry analysis. The numbers of CFSE^{high} and CFSE^{low} were counted, and the *in vivo* $OVA_{257-264}$ specific lysis percentage was calculated according to a published equation:

$$\%\ \text{specific lysis} = \frac{\{\text{CFSE}^{low} \times x - \text{CFSE}^{high}\}}{\text{CFSE}^{low} \times x}$$

where $x = \frac{\text{CFSE}^{high}}{\text{CFSE}^{low}}$ from naive mice.

Immunofluorescence in tumor

Briefly, 15 μm-thick sections at intervals of 100 μm were obtained using a freezing microtome (Leica, Germany) and mounted on poly-L-lysine-coated slides. The sections were washed in PBS and then blocked with 10% goat serum at room temperature for 1 h. CD8$^+$ T cells were defined using FITC-conjugated rat-anti-mouse CD8a antibody (BioLegend, San Diego, CA). MDSCs were defined using FITC-conjugated rat-anti-mouse CD11b antibody and APC-conjugated rat-anti-mouse Gr1 antibody (BioLegend, San Diego, CA). The nuclei were stained with DAPI. Images were taken using confocal laser-scanning microscopy (Zeiss, Germany). To further evaluate the antitumor effect of YSL-OVA formulations on the animals, the tumors were fixed with 4% (v/v) paraformaldehyde in PBS (pH 7.4) and sectioned into 15 μm slices. Apoptotic and non-apoptotic cells in tumor tissues were histologically evaluated with hematoxylin and eosin (H&E) staining and with a terminal deoxynucleotidyl transferase-mediated nick end labeling (TUNEL) assay, using a commercial apoptosis detection kit (Roche). TUNEL-positive (apoptotic) cells had pyknotic nuclei with red fluorescent

staining. Images of the sections were taken with a fluorescence microscope (Nikon, Tokyo, Japan).

Flow cytometric evaluation of single-cell suspensions in tumor and spleen

Tumor-infiltrating and splenic lymphocytes were analyzed by flow cytometry. In brief, tumor and spleen tissues were harvested and digested with collagenase D and DNase I at 37 °C for 60 min. After lysis of the red blood cells (RBCs), the dissociated cells were dispersed in 2 mL of PBS. The tumor infiltrating $CD8^+/CD4^+$ T cells and MDSC ($CD11b^+Gr1^+$) cells were stained with the following fluorescence-labeled antibodies: PE/Cy7-CD3 antibody, FITC-CD4 antibody, Percp-CD8a antibody, FITC-CD11b and APC-Gr1 antibody, respectively. Meanwhile, to test the effect of YSL-OVA on the proportion of $CD4^+/IL\text{-}4^+/IFN\text{-}\gamma^+$ cells in the splenocytes, the cells (5×10^6) were incubated with or without 10 μM OVA at 37 °C for 24 h.

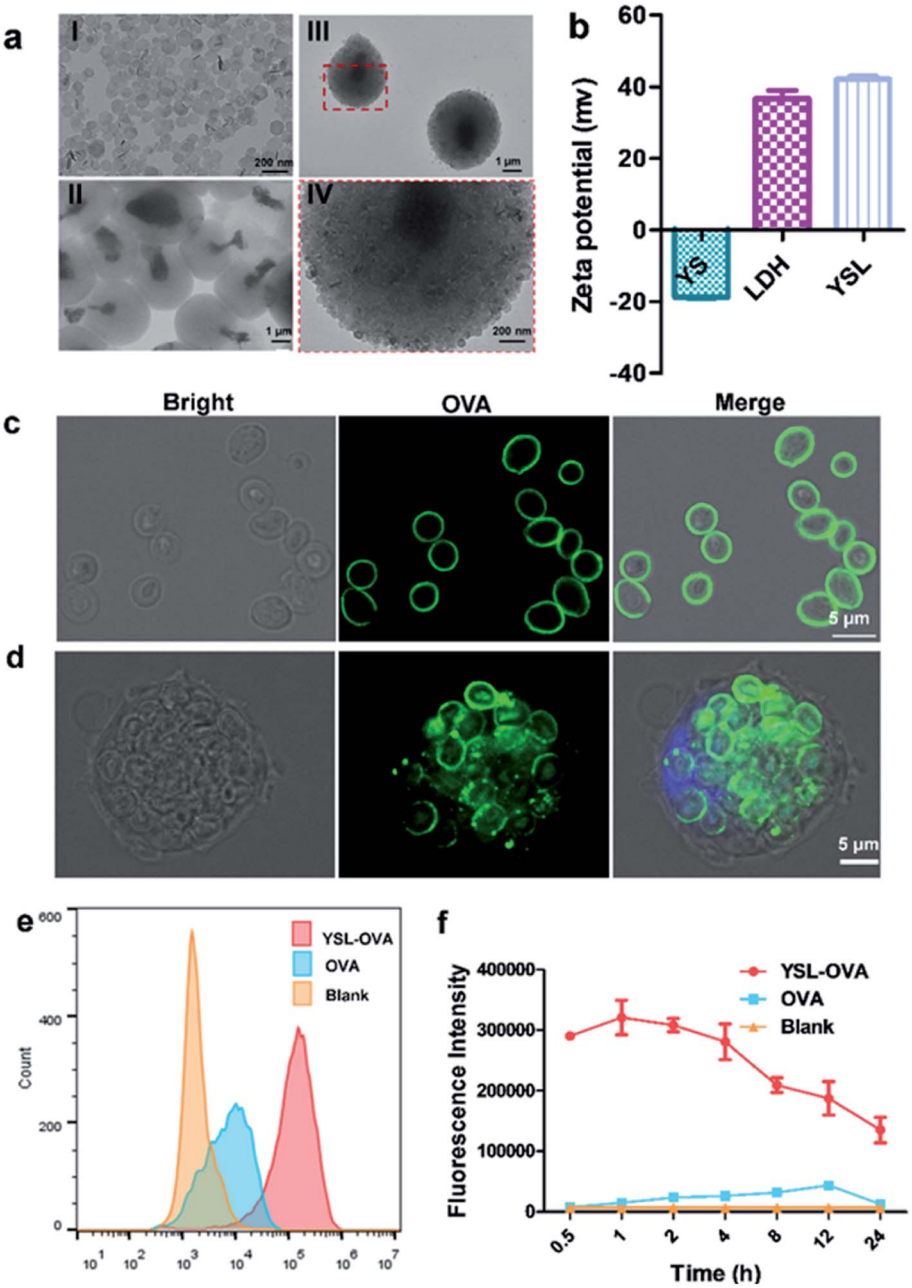

Fig. 2 Characterization of YSL particles and uptake by BMDCs. YSL particles were obtained by direct assembly of LDH on the surface of yeast shell particles in a single step. (a) The morphologies of LDH (I), yeast shell (YS) (II) and YSL (III and IV) were observed by TEM. (b) Zeta potential of yeast shell, LDH and YS-LDH. (c) YSLs were incubated with FAM-OVA for 30 min at RT to prepare YSL-OVA, and their images were obtained by CLSM. (d) BMDCs were incubated with YSL-OVA for 4 hours and then imaged by confocal laser scanning microscopy. (e and f) BMDCs were incubated with YSL-OVA at 37 °C for different times. The mean fluorescence intensity (MFI) of BMDCs was detected with a flow cytometer.

Brefeldin A (BioLegend, 1 : 1000 dilution) was added to prevent extracellular secretion, and the cultures were incubated for a further 4 h. Splenocytes were resuspended in staining buffer and incubated with the antibodies against CD3 (PE/Cy7-labelled), CD4 (FITC-labelled), IL-4 (PE-labelled) and then IFN-γ (APC-labelled). Proportions of $CD4^+$/IFN-γ^+ cells and $CD4^+$/IL-4^+ in $CD3^+$ T cells were determined by BD Arial III flow cytometry (BD, USA).

To test the ability of YSL-OVA to stimulate the production of OVA-specific cytokine in mouse spleen, the splenocytes (5×10^6 per well) from immunized mice were incubated with or without OVA (20 μM) in 24-well culture plates at 37 °C for 72 h. The culture supernatant was collected and the concentration of IFN-γ, IL-10, IL-17A, TNF-α and IL-6 was determined by a LEGENDplex™ Mouse Proinflammatory Chemokine Panel Mix (BioLegend, San Diego, CA).

Safety evaluation

C57BL/6 mice were injected subcutaneously with PBS or YSL, and the blood of the mice was collected at 6 h, 24 h, 4 days and 7 days post administration. Concentrations of IL-6 were assayed by ELISA (Neobioscience, China). At the same time, white blood cell, red blood cell and platelet counts from the blood were detected using Blood Routine. Several biological markers for liver/kidney/heart function were measured from the blood samples: alanine transaminase (ALT), aspartate transaminase (AST), alkaline phosphatase (ALP), blood urea nitrogen (BUN) and lactate dehydrogenase (LDH).

Statistical analysis

Data were analyzed by one-way analysis of variance, followed by multiple comparisons using Tukey's test in GraphPad Prism 6

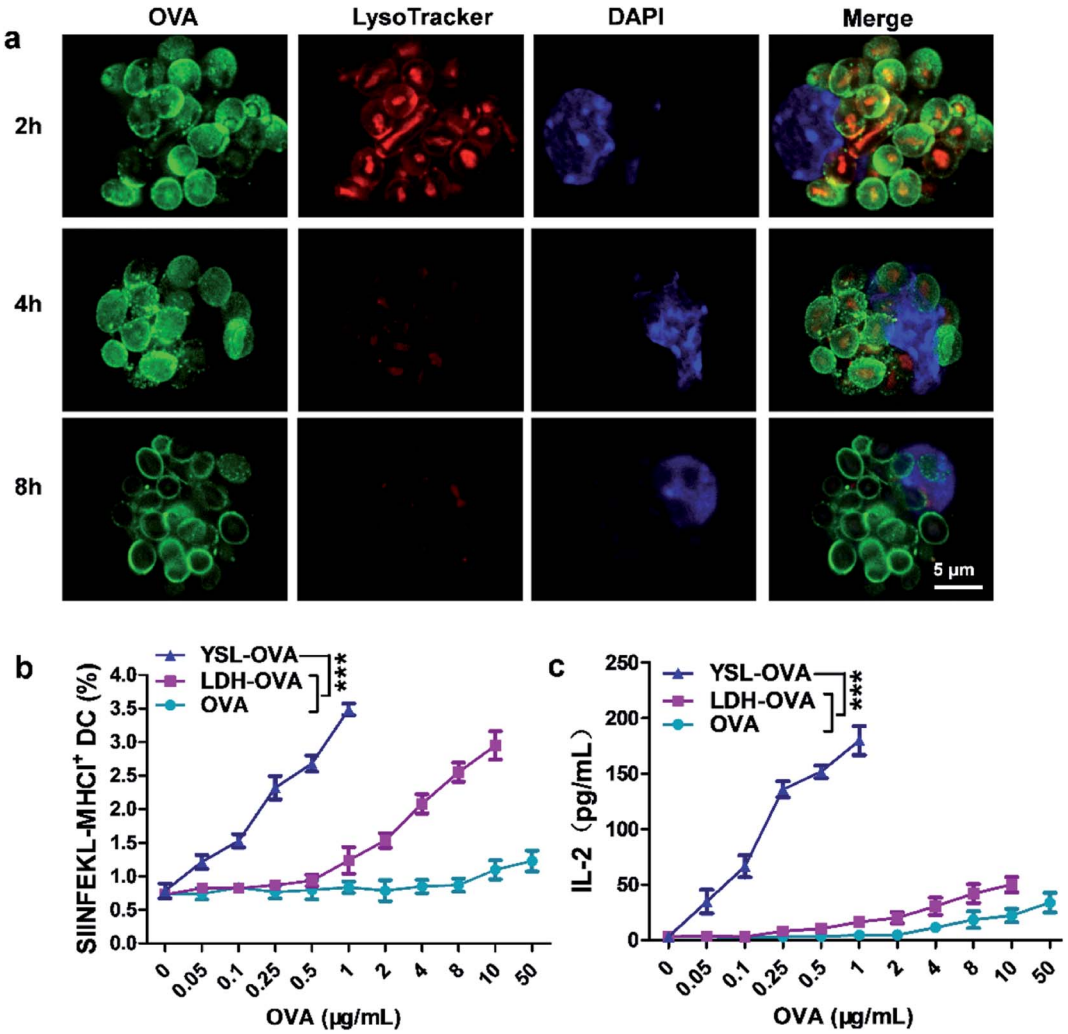

Fig. 3 Intracellular tracking and cross-presentation efficiency of YSL-OVA in BMDCs. (a) Six day-cultured BMDCs were incubated with YSL-OVA at ratio 10 : 1 (YS : cell). The cells were imaged by confocal laser scanning microscopy at 4, 8 and 12 h. The OVA was labeled with FAM and phgo/lysosomal were labeled with red LysoTracker. The cell nuclei were stained with DAPI. The scale bars represent 5 μm. (b and c) Immature BMDCs were incubated at 37 °C for 24 h with free OVA, LDH-OVA (ratio = 16 : 1) or YSL-OVA (containing 10^6 YS) over the indicated OVA concentration range, then RF33.70 cells were co-incubated with dendritic cells at a ratio of 5 : 1 for 24 h. (b) The expression of SIINFEKL-$MHCI^+$ of DCs was detected by flow cytometry. (c) The amount of IL-2 from activated RF33.70 T hybridoma cells was determined by ELISA.

software. Differences were considered significant at $*p < 0.05$, $**p < 0.01$, and $***p < 0.001$.

Results and discussion

Preparation and characterization of the biomimetic YSL particles

The glucan particles were characterized by their ellipsoidal "wrinkled pea" morphology and irregular delineation with protein and DNA removed by consecutive alkali and acid treatments (Fig. S1†). Clay LDH nanoparticles were prepared as in a previous report.[28] TEM results and laser diffraction measurement showed that clay LDH nanoparticles were around 100 nm in diameter with a zeta-potential of +35.0 ± 1.5 mV (Fig. 2aI and b), and the yeast shell (YS) had an average diameter of 2–4 μm with a zeta-potential of −18.0 ± 0.6 mV (Fig. 2aII and b). Hence, the positively charged LDH nanoparticles were absorbed onto the negatively charged yeast shell *via* Coulomb force. Accordingly, the zeta potential of the YSLs increased from −18 mV to +40 mV after the LDH nanoparticles were absorbed on the surface of YS. The morphology of the prepared YSL particles was further observed *via* TEM. Similar to the original YS particles, TEM results showed that YSL had a uniform particle size of approximately 2–4 μm (Fig. 2aIII and IV). Moreover, the naked yeast cell wall had a smooth surface, whereas the YSL surface exhibited numerous LDH nanoparticles (Fig. 2aIV), which increased the antigen loading capability due to the large specific area and positive charge on their surface.

YSLs promoted the uptake of antigen *via* BMDCs

As shown in Fig. 2c, confocal laser scanning microscopy (CLSM) results showed that the OVA protein was intensively absorbed on the surface of the YSLs, which simulated the dense and repetitive antigen distribution on the surface of natural microorganisms. Yeast shell, mainly made of β-glucan that is a danger signal for APCs, may mimic a pathogen structure to induce the phagocytosis of antigens by APCs. LDH with a high antigen-loading capacity facilitates antigen delivery to APCs, and induces antigen endosome escape and cross-presentation.[24] The LDH contents determined in YSL particles were 30 ± 2.1%, and the loading capacity was determined by measuring the remaining protein in the supernatant with BCA, and a loading capacity of approximately 10% (100 μg OVA protein/1 mg YSL-OVAs) was obtained with this simple mixing procedure. When YSLs were incubated with BMDCs, a large number of YSL-OVA particles were swallowed by the BMDCs (Fig. 2c and d). YSL-OVA particle uptake by BMDCs was further quantified with the mean fluorescence intensity (MFI) of FAM using flow cytometry at 0.5, 1, 2, 4, 8, 12, and 24 h, respectively (Fig. 2e and f). The YSL-loaded OVA were phagocytosed by BMDCs at an extremely high rate after 30 min, and over 300-fold uptake of YSL-OVA at 1 h was observed in BMDCs compared with the uptake of free OVA. Moreover, OVA remained in the cell for more than 24 hours. These results suggested that YSL particles greatly enhanced the intracellular delivery of OVA to DCs (Fig. 2f). It is worth mentioning that the phagocytized YSLs

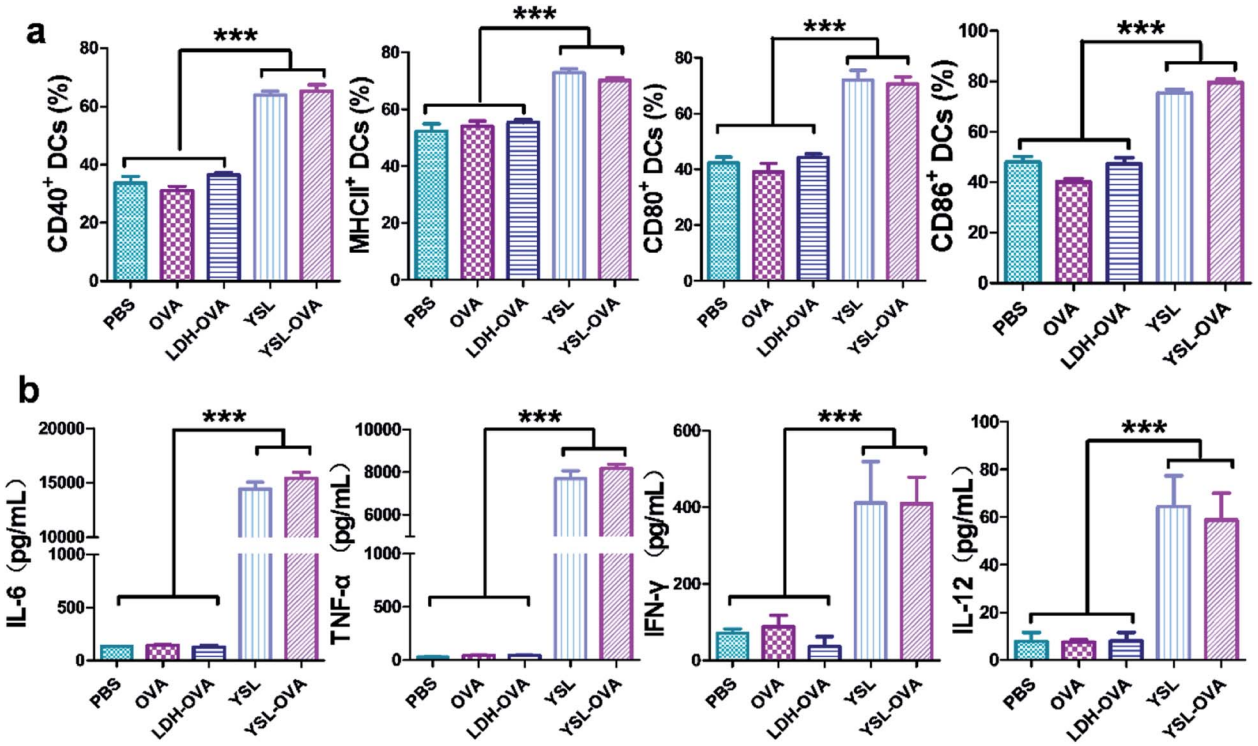

Fig. 4 BMDC maturation and cytokine production stimulated by YSL-OVA particles. (a) BMDCs were incubated with free OVA, LDH-OVA, YSL and YSL-OVA (YSL : cell = 10 : 1) at 37 °C for 48 h, the cells were stained with anti-mouse CD40, MHCII, CD80 and CD86 antibodies, and the expression levels of co-stimulatory molecules were analyzed by flow cytometry. (b) The levels of IL-6, TNF-α, IFN-γ and IL-12 in the supernatant were measured by ELISA. Data shown are the mean ± SD ($n = 4$), $*p < 0.05$, $**p < 0.01$, $***p < 0.001$.

exhibited little influence on the viability of BMDCs (Fig. S2†), although drastic internalization occurred.

YSL vaccine promoted DC cross-presentation and stimulated antigen specific CD8 T cell activation

To further investigate the intracellular tracking of YSL, the OVA was labeled with the green fluorescence dye FAM. After incubating YSL-OVA with BMDCs at a ratio of 10 : 1 (YSL : cell) for 2 h, the phagosomes were labeled with LysoTracker and stained by LAMP-1. The confocal laser scanning microscopy results showed that most YSLs were co-localized with lysosomes after 2 h of incubation (Fig. 3a and S3†). Interestingly, when the incubation time was extended, the lysosomes gradually disappeared from 4 to 8 h (Fig. 3a), which is consistent with a previous report that LDH significantly neutralized endosomal and lysosomal acidity in cells through partial dissolution, leading to quick lyosomal escape.[24]

Next, we evaluated whether YSL-OVA-induced DC activation could stimulate antigen specific CD8 T cell proliferation. Compared with DCs pulsed with soluble OVA, DCs treated with LDH-OVA more efficiently presented epitope peptides (SIINFEKL, $OVA_{257-264}$) *via* the major MHC I-restricted pathway (Fig. 3b), suggesting that the LDH-mediated intracellular trafficking pathway induced effective cross-presentation. Surprisingly, YSL-OVA particles exhibited the most robust upregulation of the SIINFEKL-MHC I complex at an OVA concentration from 0.05 to 0.5 μg mL^{-1} which is 100-fold less than that of free OVA, demonstrating efficient antigen delivery and dispersion in the cytoplasm mediated by YSLs (Fig. 3b).

To detect the effect of stimulated DC on CD8 T cell activation, DCs pulsed with various. OVA vaccines were incubated with murine T cell hybridoma cells which recognize $OVA_{257-264}$ (RF33.70), and the resultant IL-2 concentration in the supernatant was measured. As shown in Fig. 3c, LDH-OVA and free OVA solutions elicited only weak T-cell proliferation at concentrations of 10 μg mL^{-1} and 50 μg mL^{-1}, respectively. As expected, DCs incubated with YSL-OVA particles significantly improved T cell stimulation even when the OVA concentration was much lower, demonstrating that the yeast shell and LDH synergistically induced effective CD8 T activation.

YSL particles potently activated DCs

We next evaluated the effect of YSL on DC activation and maturation. Yeast shell strongly activated DC maturation by the interaction of β-glucan with TLR-2, TLR-6 and dectin-1.[29] The flow cytometry results in Fig. 4a show that co-stimulatory molecules CD40, CD80 and CD86 and the MHC II level were significantly upregulated in the YSL-OVA and YSL-treated groups. However, LDH-OVA did not increase the expression of these markers. CD40 and CD80/86 provide the costimulatory signals necessary for T-cell activation and survival,[30] while MHC

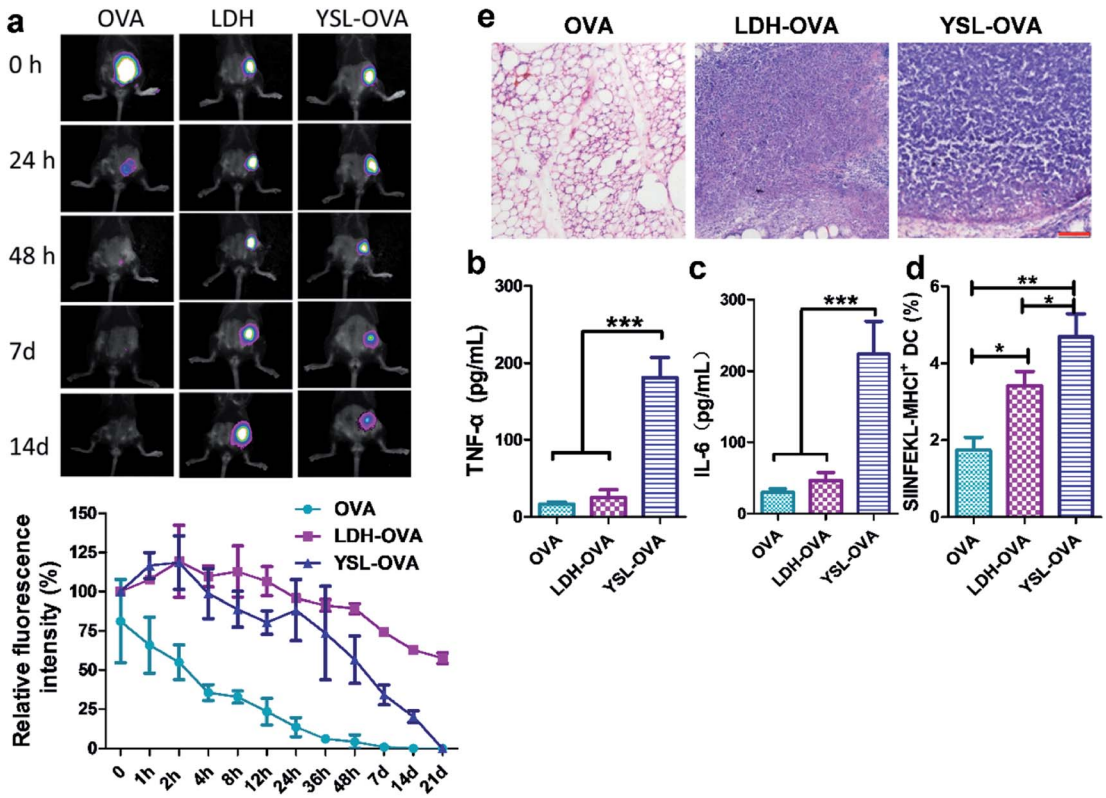

Fig. 5 Local antigen preservation and immune response at injection sites. C57BL/6 mice were subcutaneously injected with the indicated formulations. (a) OVA was labelled with Cy5. Fluorescent intensity of antigen persistence was detected over the indicated time. (b and c) Inflammatory cytokines level of TNF-α (b) and IL-6 (b) at injection sites. (d) Flow cytometry analysis of SIINFEKL-$MHCI^+$ of recruited DCs 48 h post administration in draining lymph nodes. (e) The monocyte infiltration at the injection site 48 h after administration. The antigen depots were sectioned and then dyed with H&E. Scale bar is 200 μm. Data shown are the mean ± SD ($n = 4$), *$p < 0.05$, **$p < 0.01$, ***$p < 0.001$.

II is involved in antigen presentation to CD4 activation, benefiting the activation of B cells and CD8 T cells.[31,32]

Inflammatory cytokines such as TNF-α, IL-6, IFN-γ, and IL-12 play an important role in the immune reaction. Cytokine secretion of the DCs stimulated by YSL-OVA and YSL were measured by ELISA. After incubation with the particles for 48 h, the YSL-OVA or YSLs greatly enhanced the levels of secreted TNF-α, IL-6, IFN-γ and IL-12 in the cell supernatant (Fig. 4b), suggesting that YSLs were favorable stimulators for the Th1 and Th2 immune response.

Antigen preservation and APC trafficking of YSL vaccine *in vivo*

To investigate the *in vivo* fate of antigens on YSL, the same amounts of Cy5 labeled OVA (20 μg Cy5-OVA) in all formulations were subcutaneously injected into the groins of the mice. As shown in Fig. 5a, the fluorescence signal of free Cy5-OVA was nearly undetectable at 24 h after administration, while the fluorescence intensity of LDH-OVA and YSL-OVA remained strong at the injection site 48 h after injection. Cy5-OVA was rapidly released from YSL-OVA particles in the early phase, with 56.6 ± 6.7% remaining in the depot after 48 h, then released slowly with 20% ± 3.3% remaining in the depot after 14 d, and was cleared after 21 d, whereas the Cy5-OVA was very slowly released from the agglomerates formed by LDH, with 89.2% ± 2.1% at 48 h and 57.6 ± 3.1% at 21 d remaining in the depot, suggesting that antigen delivered by YSLs could avoid antigen rapid degradation and diffusion with maximum antigen utilization during the vaccinized term.

The inflammatory factors in the antigen depots are vital to activate APC maturation,[33] and the secretions of TNF-α and IL-6 were significantly increased by YSLs to 185.8 ± 15.6 pg mL^{-1} and 201.8 ± 11.5 pg mL^{-1} in the YSL-OVA vaccine depot, respectively (Fig. 5b and c), indicating that YSL created a pro-inflammatory environment for triggering the potential chemokine-driven influx of antigen-presenting cells. As a result,

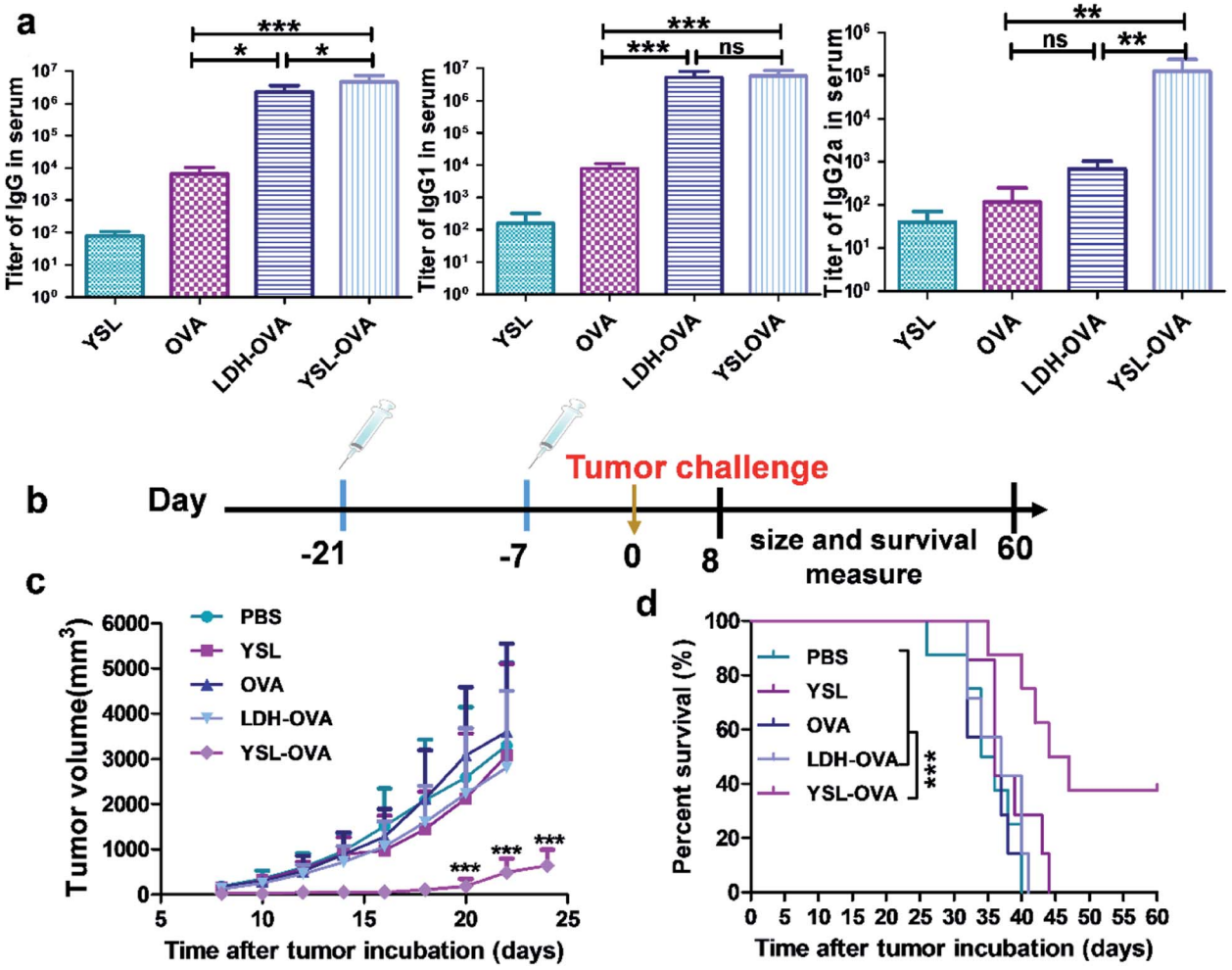

Fig. 6 YSL vaccine prophylactically inhibits tumor growth *in vivo*. C57BL/6 mice were subcutaneously immunized with various vaccines, as described in the text. Blood was withdrawn for analysis of humoral and cellular immune responses seven days after the secondary immunization. (a) ELISA results of the OVA-specific antibody titers. (b) Schematic showing the anti-tumor immunity in a prophylactic tumor model. (c and d) YSL-OVA immunization protected mice from challenge with E.G7-OVA tumor. C57L/B6 mice were s.c injected with 1×10^6 E.G7-OVA tumor cells 14 days after the last immunization. Tumor volume (c) and the survival time of tumor-bearing mice (d) were measured. Data shown are the mean ± SD ($n = 8$), *$p < 0.05$, **$p < 0.01$, ***$p < 0.001$.

many more APCs were distinctively recruited to the YSL-OVA vaccination site compared to those of free OVA or LDH-OVA (Fig. 5e). Furthermore, *in vivo* tracking showed that after their activation by the YSL-OVA vaccine, the antigen primed DCs more efficiently migrated to the draining lymph nodes (LNs) than those driven by solely OVA or LDH-OVA groups (Fig. 5d), where DC can interact with T cells, promoting stronger antigen-specific CTL responses.

We also investigated the biosafety of YSL by detecting the physiological characteristics in mice during 7 consecutive days. The results showed that the IL-6 level in the serum from YSL vaccination significantly increased compared with the control at an early stage (6–24 h), but then reached the normal range after 4 days (Fig. S7†). Meanwhile, the blood routine analysis demonstrated that there was no significant difference between YSL and control on the number of white blood cells, red blood cells and platelets. Hepatic, renal and cardiac function were further evaluated using the serum of mice after treatment. No significant difference was observed for the levels of biochemical parameters AST, ALT, ALKP, BUN and LDH (Table S2†), suggesting that YSL particles have a certain biosafety *in vivo*.

YSL-OVA vaccine as a prophylactic vaccine inhibited tumor cell growth *in vivo*

We next examined the ability of the YSL-OVA particles to induce antigen-specific immune responses *in vivo*. An ideal cancer vaccine delivery system should effectively activate $CD8^+$ as well as $CD4^+$ T cells to promote the activation of CTLs and B cells, respectively.[34,35] As shown in Fig. 6a, YSL-OVA particles induced robust antigen specific total IgG titers, with strong preference

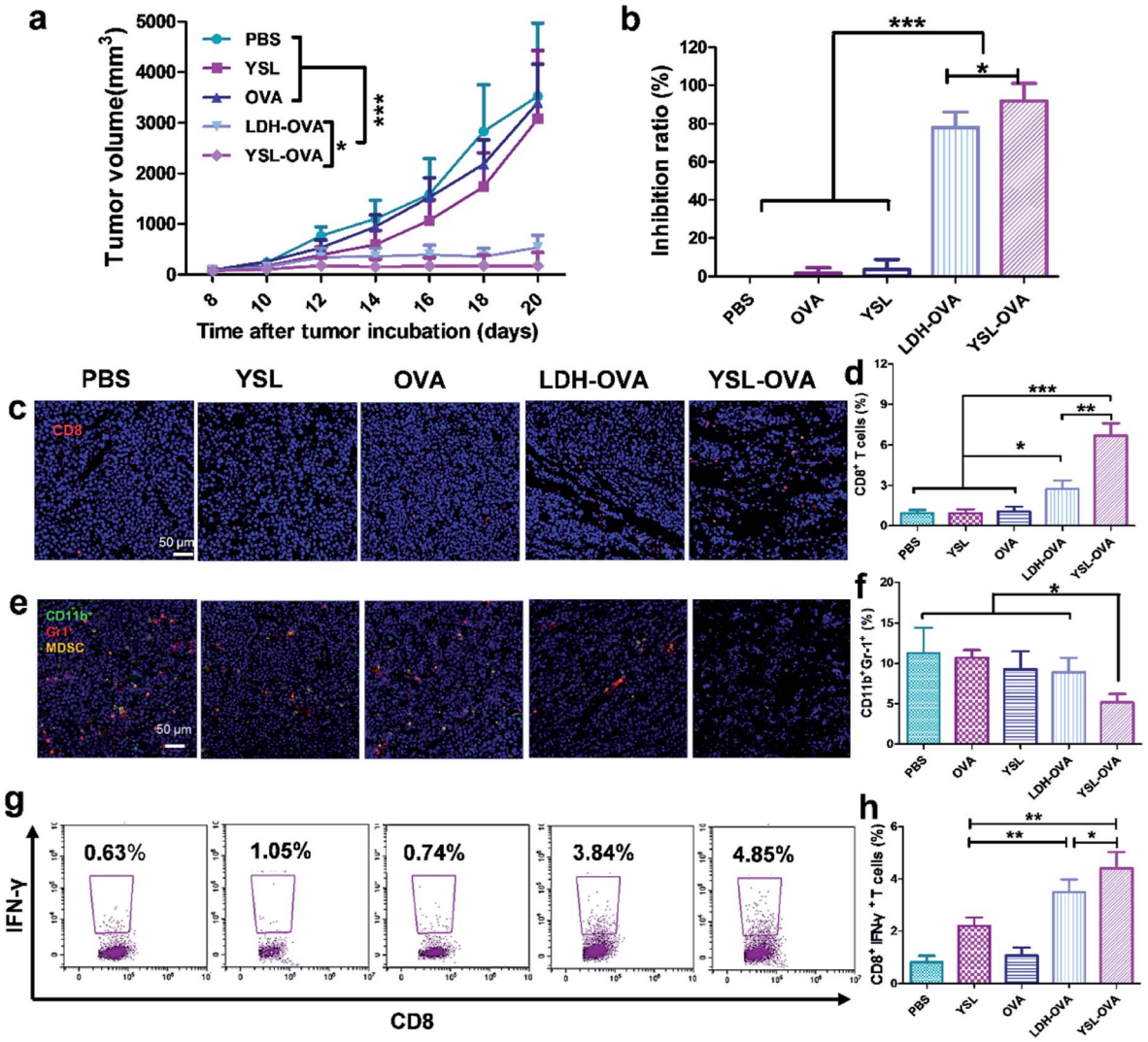

Fig. 7 YSL vaccine exerts robust therapeutic effects towards E.G7-OVA lymphoma. (a) Mice were inoculated with 1×10^6 E.G7-OVA lymphoma cells on day 0. Animals were injected subcutaneously with different vaccine formulations on days 4 and 11. Tumor volume was monitored every 2 days and calculated. (b) The tumor inhibition ratio was calculated based on the weight of the tumor at the end of the tests. $CD11b^+/Gr1^+$ MDSC cells (c and d) and $CD8^+$ T cells (e and f) in tumor tissues were assayed with immunofluorescence staining and flow cytometric analysis. (g and h) Flow cytometry evaluation of the cellular immune responses in the tumor by means of the frequency of IFN-γ-secreting $CD8^+$ T cells in the tumor. Results are shown as mean ± SD ($n = 7$), *$p < 0.05$, **$p < 0.01$, ***$p < 0.001$.

for subtypes IgG1 and IgG2a. Compared with YSL-OVAs, LDH-OVA also triggered a strong IgG titer. However, a bias towards IgG1 and almost no IgG2a titers were observed after immunization. Since the antibody IgG2a isotype is supposed to be a marker of Th1 type immune responses, our results indicated that YSL-OVAs induced strong humoral and Th1-type immune responses. To further assess the immune protection, mice were subsequently challenged with E.G7-OVA lymphoma cells 14 days after the prime-boost immunization. In all groups, YSL alone showed a slight anti-tumor effect, suggesting a benefit from the activation of innate immune cells. Excitingly, the average tumor volume in mice vaccinated with YSL-OVA was considerably smaller than that in the other groups at all time points (Fig. 6c), whereas LDH-OVA did not exert an obvious immune protection by its Th2 bias immune response in the prophylactic vaccine model. Accordingly, YSL-OVA significantly increased the survival of mice compared with other vaccines (Fig. 6d).

YSL-OVA particles exerted robust therapeutic tumor effects

We next assessed the therapeutic efficacy of YSL-OVA towards established tumors. Mice were inoculated with 1×10^6 E.G7-OVA lymphoma cells and vaccinated with the indicated formulations on days 4 and 11. As shown in Fig. 7a, b and S4,† the LDH-OVA and YSL-OVA groups significantly delayed the tumor growth relative to free OVA treatment. Among all groups, maximum tumor growth inhibition up to ~91.8% was achieved by YSL-OVA vaccination. These results demonstrated that LDH and yeast shell exerted synergistic action on anti-tumor efficacy.

Tumor tissues from PBS, YSL and OVA treated groups appeared hypercellular and exhibited nuclear polymorphism, while the tumor tissues from the mice vaccinated with YSL-OVA displayed bulk necrosis and acellular regions (Fig. S5a†). The TUNEL apoptosis assay also showed the highest level of cellular apoptosis in the YSL-OVA treated group (Fig. S5b†). These results indicated that the YSL-OVA vaccine induced the most efficient immune response relative to other groups.

YSL-OVA vaccine changed the populations of immune cells in a tumor

To examine the effect of YSL-OVA particles on the proportions of immune cells in a tumor, the mice were vaccinated with various vaccine formulations, and the tumors were extracted 21 days after immunization. The infiltrating $CD8^+$T and immune inhibitory MDSCs were analyzed by immunofluorescence and flow cytometry, respectively. LDH-OVA and YSL-OVA treatments significantly increased the $CD8^+$ T cell level in the tumor, as shown in Fig. 7c and d (2.74% and 6.68%, respectively). Moreover, as a prerequisite for cellular immunity, YSL-OVA induced the highest proportion of IFN-γ-secreting $CD8^+$ T cells (4.41%,

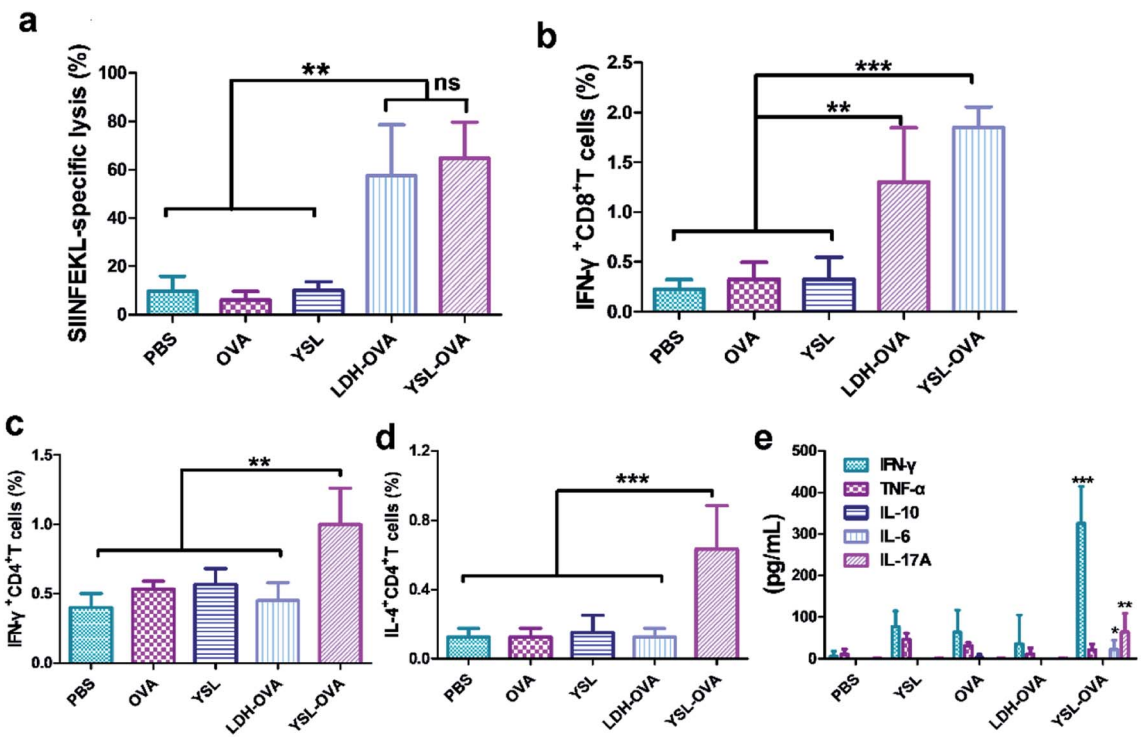

Fig. 8 YSL vaccine induces both $CD8^+$ and $CD4^+$ T cell anti-tumor immunity. (a) Splenocytes from naive mice were pulsed with PBS or OVA peptide (SIINFEKL) and stained with low (PBS) or high (OVA) concentrations of CFSE, respectively. The cells were then mixed and injected i.v. into the vaccinated mice. After 18 h, splenocytes from the vaccinated mice were analyzed by flow cytometry and enumerated according to a published equation. (b–e) Splenocytes were isolated from various vaccinated mice and pulsed with OVA protein or medium for 72 h. The cells were then collected and stained with antibodies against IFN-γ^+ $CD8^+$ (b), IFN-γ^+CD4^+ (c) and IL-4^+CD4^+ (d), and then detected by flow cytometry. (e) The release profiles of the representative cytokines for the T helper cells, IFN-γ, TNF-α, IL-10, IL-6 and IL-17A, in the supernatant were detected using ELISA kits, respectively. Results are shown as mean ± SD ($n = 4$). *$p < 0.05$, **$p < 0.01$, ***$p < 0.001$.

Fig. 7g and h) compared with other groups. In tumor-bearing hosts, myeloid-derived suppressor cells (MDSCs) play important roles in immune suppression, and the reversal of their function is vitally important for the success of an immune therapy.[36] Treatment groups that received YSL-OVA treatment showed a significant drop in the presence of intratumoral MDSCs compared with the other groups in Fig. 7e and f (5.16%, $P < 0.05$), indicating the ability of YSL-OVA vaccine to improve the tumor's immune suppression.

YSL-OVA vaccine induced robust CTL and Th1/Th17 mix cellular immune responses

In the therapeutic tumor model, cellular immune responses are essential for cancer therapy, so we then assessed the antigen-specific CTL responses in the vaccinated mice using an *in vivo* CTL evaluation method. Mice treated with PBS, YSL or free OVA did not exhibit any noticeable OVA-specific CTL response. In contrast, mice treated with LDH-OVA and YSL-OVA efficiently eliminated ~57.6% and 64.9%, respectively, of OVA peptide-pulsed target cells, compared with OVA alone (9.2% ± 2%, $p < 0.01$) (Fig. 8a and S6†).

We next investigated the cellular immune responses evoked by YSL-OVA vaccine *via* measurement of CD8 and CD4 T cell activation. The flow cytometry results in Fig. 8b showed that LDH-OVA and YSL-OVA treatment significantly increased the proportion $CD8^+/IFN\text{-}\gamma^+$ cells by 400% and 569%, respectively, compared with the free OVA group. Moreover, YSL-OVA also induced robust cellular immune reactions with a higher population of IFN-γ- and IL-4-secreting $CD4^+$ T cells than the other vaccines (Fig. 8c and d), demonstrating that YSL-OVA rapidly induced potent Th1- and Th2-mediated responses. However, the LDH-OVA treatment did not exhibit any noticeable OVA-specific $CD4^+$ T response. Accumulating data demonstrates that Th17 cells play an important anti-tumor role, particularly in the immune responses with combined Th1/Th17 responses and IFN-γ production.[5,37,38] Interestingly, the data in Fig. 8e showed that the YSL-OVA group significantly induced IL-17 production, further indicating potent Th1-, Th17- and Th2-mediated responses induced by YSL-OVA, indicating that YSL-OVA vaccine exerted comprehensive immune responses.

Conclusion

In summary, we have here developed a facile, green synthesis of a yeast shell-LDH hybrid particulate system as a vaccine carrier to co-deliver antigen and adjuvant by mimicking the morphology and danger signals on a natural microorganism surface, enhancing antigen loading capacity and stimulating an immune response. Their optimal size and surface characteristics help YSL particles specifically target APCs, strongly inducing DC maturation and cytokine secretion. The system enhanced antigen cross-presentation elicited strong CTL and Th1/Th17 activity, and stimulated intense humoral and cellular immune responses, as well as prophylactic and therapeutic effects against tumors. YSL as a general platform can be used for the preparation of cancer vaccines and other types of vaccines to stimulate strong humoral or cellular immune responses.

Conflicts of interest

There are no conflicts to declare.

Acknowledgements

We are grateful for grants from the National Natural Science Foundation of China [31401158, 81972444].

References

1 W. J. Lesterhuis, J. B. A. G. Haanen and C. J. A. Punt, *Nat. Rev. Drug Discovery*, 2011, **10**, 591–600.
2 I. Melero, G. Gaudemack, W. Gerritsen, C. Huber, G. Parmiani, S. Scholl, N. Thatcher, J. Wagstaff, C. Zielinski, I. Faulkner and H. Mellstedt, *Nat. Rev. Clin. Oncol.*, 2014, **11**, 509–524.
3 G. Zeng, Y. Li, M. El-Gamil, J. Sidney, A. Sette, R. F. Wang, S. A. Rosenberg and P. F. Robbins, *Cancer Res.*, 2002, **62**, 3630–3635.
4 J. Borst, T. Ahrends, N. Babala, C. J. M. Melief and W. Kastenmuller, *Nat. Rev. Immunol.*, 2018, **18**, 635–647.
5 J. Terhune, E. Berk and B. J. Czerniecki, *Vaccines*, 2013, **1**, 527–549.
6 Z. S. Yang, M. M. Xu, Z. H. Jia, Y. T. Zhang, L. Wang, H. R. Zhang, J. Y. Wang, M. Song, Y. P. Zhao, Z. Z. Wu, L. Q. Zhao, Z. N. Yin and Z. Y. Hong, *Biomaterials*, 2017, **134**, 51–63.
7 B. Guy, *Nat. Rev. Microbiol.*, 2007, **5**, 505–517.
8 Y. Pan, X. P. Li, T. Y. Kang, H. Meng, Z. L. Chen, L. Yang, Y. Wu, Y. Q. Wei and M. L. Gou, *Sci. Rep.*, 2015, **5**, 10687.
9 M. Aouadi, G. J. Tesz, S. M. Nicoloro, M. Wang, M. Chouinard, E. Soto, G. R. Ostroff and M. P. Czech, *Nature*, 2009, **458**, 1180–1184.
10 B. N. Gantner, R. M. Simmons, S. J. Canavera, S. Akira and D. M. Underhill, *J. Exp. Med.*, 2003, **197**, 1107–1117.
11 G. D. Brown, P. R. Taylor, D. M. Reid, J. A. Willment, D. L. Williams, L. Martinez-Pomares, S. Y. C. Wong and S. Gordon, *J. Exp. Med.*, 2002, **196**, 407–412.
12 H. B. Huang, G. R. Ostroff, C. K. Lee, C. A. Specht and S. M. Levitz, *Mbio*, 2010, **1**, e00164-10.
13 R. De Smet, T. Demoor, S. Verschuere, M. Dullaers, G. R. Ostroff, G. Leclercq, L. Allais, C. Pilette, M. Dierendonck, B. G. De Geest and C. A. Cuvelier, *J. Controlled Release*, 2013, **172**, 671–678.
14 S. Yan, B. E. Rolfe, B. Zhang, Y. H. Mohammed, W. Gu and Z. P. Xu, *Biomaterials*, 2014, **35**, 9508–9516.
15 A. Jegerlehner, T. Storni, G. Lipowsky, M. Schmid, P. Pumpens and M. F. Bachmann, *Eur. J. Immunol.*, 2002, **32**, 3305–3314.
16 M. B. Bernstein, M. Chakraborty, E. K. Wansley, Z. Guo, A. Franzusoff, S. Mostbock, H. Sabzevari, J. Schlom and J. W. Flodge, *Vaccine*, 2008, **26**, 509–521.

17 Z. P. Xu, Q. H. Zeng, G. Q. Lu and A. B. Yu, *Chem. Eng. Sci.*, 2006, **61**, 1027–1040.
18 W. M. Kriven, S. Y. Kwak, M. A. Wallig and J. H. Choy, *MRS Bull.*, 2004, **29**, 33–37.
19 T. Nakamura, K. Ono, Y. Suzuki, R. Moriguchi, K. Kogure and H. Harashima, *Mol. Pharmaceutics*, 2014, **11**, 2787–2795.
20 L. Y. T. Chou, K. Ming and W. C. W. Chan, *Chem. Soc. Rev.*, 2011, **40**, 233–245.
21 M. L. Lin, Y. Zhan, A. I. Projetto, S. Prato, L. Wu, W. R. Heath, J. A. Villadangos and A. M. Lew, *Proc. Natl. Acad. Sci. U. S. A.*, 2008, **105**, 3029–3034.
22 Y. F. Xia, J. Wu, W. Wei, Y. Q. Du, T. Wan, X. W. Ma, W. Q. An, A. Y. Guo, C. Y. Miao, H. Yue, S. G. Li, X. T. Cao, Z. G. Su and G. H. Ma, *Nat. Mater.*, 2018, **17**, 187–194.
23 Z. P. Xu, M. Niebert, K. Porazik, T. L. Walker, H. M. Cooper, A. P. J. Middelberg, P. P. Gray, P. F. Bartlett and G. Q. Lu, *J. Controlled Release*, 2008, **130**, 86–94.
24 W. Y. Chen, B. Zhang, T. Mahony, W. Y. Gu, B. Rolfe and Z. P. Xu, *Small*, 2016, **12**, 1627–1639.
25 W. Y. Chen, H. L. Zuo, B. Li, C. C. Duan, B. Rolfe, B. Zhang, T. J. Mahony and Z. P. Xu, *Small*, 2018, **14**, e1704465.
26 L. X. Zhang, X. X. Xie, D. Q. Liu, Z. P. Xu and R. T. Liu, *Biomaterials*, 2018, **174**, 54–66.
27 Q. Zeng, H. Jiang, T. Wang, Z. Zhang, T. Gong and X. Sun, *J. Controlled Release*, 2015, **200**, 1–12.
28 W. Chen, Z. Bing, T. Mahony, W. Gu and P. X. Zhi, *Small*, 2016, **12**, 1627–1639.
29 M. Zhang, J. A. Kim and A. Y. C. Huang, *Front. Immunol.*, 2018, **9**, 341.
30 S. W. Van Gool, P. Vandenberghe, M. de Boer and J. L. Ceuppens, *Immunol. Rev.*, 1996, **153**, 47–83.
31 M. J. Bevan, *Nat. Rev. Immunol.*, 2004, **4**, 595–602.
32 S. Bedoui, W. R. Heath and S. N. Mueller, *Immunol. Rev.*, 2016, **272**, 52–64.
33 D. J. Irvine, M. A. Swartz and G. L. Szeto, *Nat. Mater.*, 2013, **12**, 978–990.
34 U. Sahin, E. Derhovanessian, M. Miller, B. P. Kloke, P. Simon, M. Lower, V. Bukur, A. D. Tadmor, U. Luxemburger, B. Schrors, T. Omokoko, M. Vormehr, C. Albrecht, A. Paruzynski, A. N. Kuhn, J. Buck, S. Heesch, K. H. Schreeb, F. Muller, I. Ortseifer, I. Vogler, E. Godehardt, S. Attig, R. Rae, A. Breitkreuz, C. Tolliver, M. Suchan, G. Martic, A. Hohberger, P. Sorn, J. Diekmann, J. Ciesla, O. Waksmann, A. K. Bruck, M. Witt, M. Zillgen, A. Rothermel, B. Kasemann, D. Langer, S. Bolte, M. Diken, S. Kreiter, R. Nemecek, C. Gebhardt, S. Grabbe, C. Holler, J. Utikal, C. Huber, C. Loquai and O. Tureci, *Nature*, 2017, **547**, 222–226.
35 J. C. Sun and M. J. Bevan, *Science*, 2003, **300**, 339–342.
36 V. Kumar, S. Patel, E. Tcyganov and D. I. Gabrilovich, *Trends Immunol.*, 2016, **37**, 208–220.
37 N. Martin-Orozco, P. Muranski, Y. Chung, X. X. O. Yang, T. Yamazaki, S. J. Lu, P. Hwu, N. P. Restifo, W. W. Overwijk and C. Dong, *Immunity*, 2009, **31**, 787–798.
38 S. Nunez, J. J. Saez, D. Fernandez, F. Flores-Santibanez, K. Alvarez, G. Tejon, P. Ruiz, P. Maldonado, Y. Hidalgo, V. Manriquez, M. R. Bono, M. Rosemblatt and D. Sauma, *Immunology*, 2013, **139**, 61–71.

